

Numerical Investigation of Wall Aerator Performance Installed in the Bottom Outlet of Seymareh Dam

Hossein Bayat¹, Mohammad Manafpour²

1- M.Sc. Graduated of Civil Engineering, Urmia University, Urmia, Iran

2- Assistant Professor in Civil Engineering, Department of Civil Engineering, Urmia University, Urmia, Iran

Email: 1- arminbayat1371@gmail.com 2- m.manafpour@urmia.ac.ir

Abstract

Nowadays, dams play a key role in supplying water for different purposes such as potable, agricultural, industrial usages, power production as well as flood control. The impeccable performance of the dams depends on the proper functioning of the related hydraulic structures such as the bottom outlets. One of the factors that can affect seriously the performance of bottom outlet is the occurrence of cavitation phenomenon downstream of the service gate as well as inside the emergency gate groove. Induced aeration of flow (using an aerator) is most efficient approach which may cause to decrease the risk of the cavitation damage. In the present study, the efficiency of wall aerator mounted on the wall of Seymareh dam's bottom outlet are numerically investigated at downstream of the service gate using FLUENT software, K- ϵ RNG turbulence model and VOF method. distribution of air concentration is studied close to the wall and bottom of conduit for various service gate openings and normal reservoir head. The results indicate that the hydraulic performance of the wall aerator is not satisfactory and air bubbles are not distributed uniformly near to the walls and their amounts are often less than 8% which is needed for avoiding the risk of cavitation damages. Geometry and location of the wall aerator are required to justify appropriately. Also installation of another aerator on the floor of conduit is proposed for reduction of cavitation hazard.

Keywords: Bottom Outlet, Wall Aerator, Two-Phase Flow, k- ϵ RNG Turbulence Model, FLUENT Software.

1. INTRODUCTION

Today, the construction of high dams has increased. In these structures, the rate of the output flow of dam outlet is high and consequently the speed is high. This high flow velocity increases the probability of cavitation at the outlets [1]. One way to reduce the risk of cavitation is Flow aeration. Because The presence of air in the area at risk of cavitation, Increases the pressure in this area [2]. In the Output of bottom outlet and after the radial gate, the aeration is often used as sudden fall-expansion [3]. The result of the research by Mohaghegh et al (2010) indicates that there are three different flow regimes in the immediate downstream of the bottom outlet service gate that limits of these regimes are different in terms of dimensionless bottom cavity length and Froude number values [1]. Critical conditions of air concentration and flow velocity to prevent cavitation damage were presented by Dong and Su (2006) [4]. Changes in pressure and cavitation index with changes in air concentration and cavitation erosion level of concrete were obtained by Dong et al (2007) [5]. Air-water flow in the curved water transfer tunnel was studied by Lee et al [7]. and the results indicate that the installation of aeration in the wall and in the transverse section can protect the lateral wall against the risk of cavitation. Numerical modeling is often used today to save time and cost. Using VOF and MIXTURE model, two-phase flow downstream of a step aeration in a water transfer tunnel was modeled by Zhang et al. (2011) [8]. Using the K- ϵ turbulence model and the VOF two-phase model, the flow was modeled after a sudden opening and floor-level drop in a under pressure water conduit by Lee et al. (2011) [9]. In this study, the two-phase flow by K- ϵ turbulence model and VOF two-phase model in FLUENT software is modeled with the aim of investigating the amount of air entered into the flow after the service gate of Seymareh dam bottom outlet, for normal reservoir head and different opening of service gate. In order to ensure the accuracy of the results, the pressure values in the floor and wall of the conduit were compared with the laboratory values. as a result, good agreement between the numerical modeling results and the experimental data was observed. Finally, using a contour of air concentration in the floor and the conduit wall, the efficiency of the wall aerator after the service gate has been judged.

2. CHARACTERISTICS OF SEYMAREH DAM AND BOTTOM OUTLET

The Seymareh Reservoir Dam has two bottom outlet in the dam body with 54.4 m long, which inlet floor level of bottom out No. 1 and No. 2 respectively is equivalent to 620 m and 640 m above sea level. Emergency gate is sliding and service gate is radial. In the present study, the bottom outlet No. 1 has been investigated for a normal head of 100 m. [10]

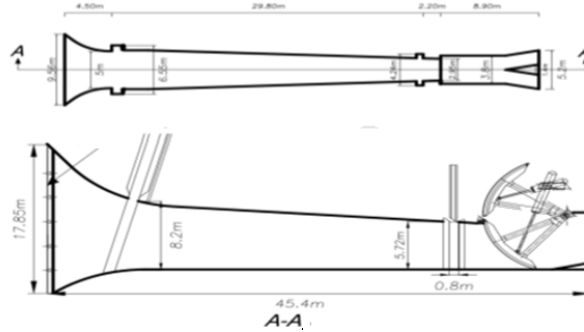


figure 1 Plan and longitudinal section of bottom outlet [10]

3. CHARACTERISTICS OF THE BOTTOM OUTLET PHYSICAL MODEL

The physical model of the bottom outlet of Seymareh Dam have been made on scale 1:15 by Tehran Water Research Institute, using Reynolds similarity of transparent sheet (plexiglass) and in parts of wood, which includes parts: inlet, middle duct, Downstream duct, emergency and service gate. To provide the required water height upstream of the bottom outlet, a metal open tank in 5 m diameter and 6 m in height was used, that at height of 6m another tank was added to it with the diameter of 2m and height of 4 m. In this model, 74 piezometers are used to measure the pressure.[10]

4. GOVERNING EQUATIONS

Continuity equation

the continuity equation for a control volume is as follows:

$$\frac{\partial}{\partial t} \int_{c.v} \rho dv + \int_{c.s} \rho \vec{v} dA = 0 \quad (1)$$

AFTER INTEGRATING:

$$\frac{\partial(\rho u)}{\partial x} + \frac{\partial(\rho v)}{\partial y} + \frac{\partial(\rho w)}{\partial z} = -\frac{\partial \rho}{\partial t} \quad (2)$$

Where w, v, u are the velocity components in the X, Y, and Z directions, respectively. According to the incompressible fluid flow, the continuity equation is as follows:

$$\frac{\partial u_i}{\partial t} = 0 \quad (3)$$

The momentum equation

By applying the Momentum survival law within a control volume, the following equation is obtained:

$$\frac{\partial}{\partial t} \oint_{\Omega} \rho \vec{V} d\Omega + \oint_{\partial\Omega} \rho \vec{V} (\vec{V} \cdot \vec{n}) dS = \oint_{\Omega} \rho \vec{f}_e d\Omega - \int_{\partial\Omega} p \vec{n} dS + \oint_{\partial\Omega} (\vec{\tau} \cdot \vec{n}) dS \quad (4)$$

Assuming an incompressible flow after simplification we have:

$$\frac{\partial u_i}{\partial t} + u_j \frac{\partial u_i}{\partial x_j} = -\frac{1}{\rho} \frac{\partial p}{\partial x_i} + g_{x_i} + \nu \nabla^2 u_i \quad (5)$$

In the above relation u_i and g_x are the components of the instantaneous velocity and the acceleration of gravity in the X_i direction, respectively, and p is pressure.

turbulence model equations:

To determine the Reynolds stress term in the momentum equation for turbulent flow, a two-K- ϵ equation model is used, which equations are as follows:

Turbulence kinetic energy equation K:

$$\frac{\partial}{\partial t}(\rho k) + \frac{\partial}{\partial x_i}(\rho k u_i) = \frac{\partial}{\partial x_j} \left[\left(\mu + \frac{\mu_t}{\sigma_k} \right) \frac{\partial k}{\partial x_j} \right] + G_k - \rho \epsilon \quad (6)$$

Turbulence kinetic energy dissipation rate equation ϵ :

$$\frac{\partial}{\partial t}(\rho \epsilon) + \frac{\partial}{\partial x_i}(\rho \epsilon u_i) = \frac{\partial}{\partial x_j} \left[\left(\mu + \frac{\mu_t}{\sigma_\epsilon} \right) \frac{\partial \epsilon}{\partial x_j} \right] + C_{1\epsilon} \frac{\epsilon}{k} G_k - C_{2\epsilon} \rho \frac{\epsilon^2}{k} \quad (7)$$

In these relationships, G_k is turbulence kinetic energy generation and μ_t is turbulence viscosity.

Free surface equation:

To determine the free surface in the VOF method, the α_q parameter is used, which denotes the fluid q value in each cell. In this method, the continuity equation for the volume ratio of the existing phases is solved. For the q phase, the continuity equation is given below:

$$\frac{\partial}{\partial t}(\alpha_q \rho_q) + \nabla \cdot (\alpha_q \rho_q \vec{v}_q) = \sum_{p=1}^n (\dot{m}_{pq} - \dot{m}_{qp}) \quad (8)$$

Where \dot{m}_{pq} is mass transfer from phase q to phase p , and \dot{m}_{qp} is mass transfer from phase p to phase q , and α_q , ρ_q and \vec{v}_q are volume ratios, density and velocity of phase q , respectively.

5. NUMERICAL MODELING

The geometry of the bottom outlet model was prepared using 3D cad software in real scale. bottom outlet geometry meshing was performed in ANSYS MESHIN software using a hexagonal element (Figure 2). Also due to the large variations of hydraulic properties around the gate and need for closer examination of them in this area, maximum mesh size, equal 0.15 m for areas away from the gate, and 0.04 to 0.08 m for around the gate was selected. The total number of computational elements for different openings varies between 300,000 and 600,000.

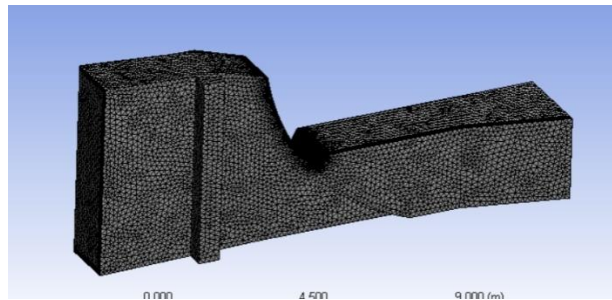


Figure 2 Bottom outlet model meshing

The solution of the flow field in the numerical model of the bottom outlet was performed in ten openings of 10% to 100% using FLUENT software. Due to the Long analysis time and saving of resources and also the importance of examining the flow in the bottom third of the bottom outlet, the onset of the flow in the numerical model was defined at a cross section with 30.7 m distance from the beginning of the bottom outlet. Due to the symmetry of the bottom outlet model with its longitudinal axis, numerical modeling was considered only for half of it (Fig. 2).

The flow in Fluent software is transiently modeled using the PRESSURE BASED solver. Also the VOF model is used to simulate water- air two-phase flow and the K- ϵ model with RNG method for turbulence modeling. The boundary conditions used in the numerical model are listed in Table (1) and flow inlet and outlet are shown in Fig 3. In the selected section as flow inlet, the value of the inlet constant velocity is considered to be

the average velocity obtained from the laboratory model at that section, which corresponds to the operation of the bottom outlet at 100 m normal head. Relative pressure equal zero was also considered at the outlet.

Table 1 Boundary conditions defined in numerical model

boundary location on the bottom outlet	boundary condition in the model
Flow inlet	Velocity inlet
Flow outlet	Pressure Outlet
conduit wall	Wall
Symmetry plane	Symmetry

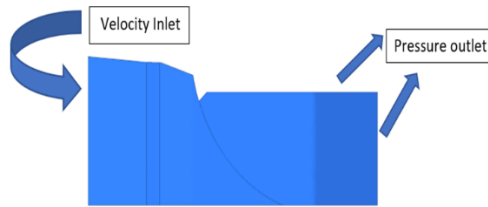
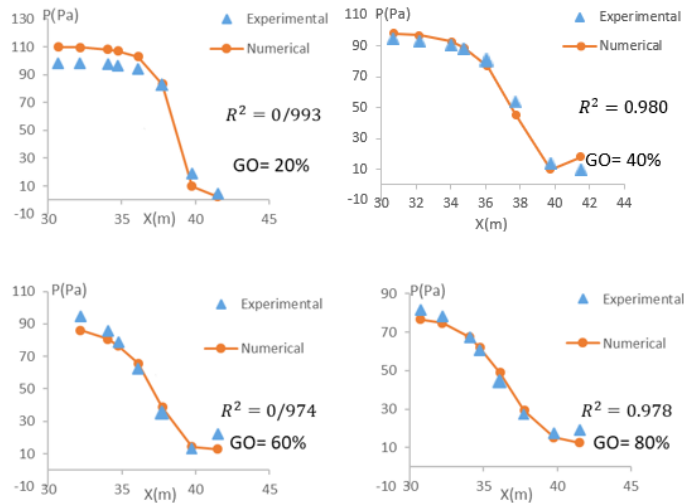


Figure 3 Inlet and Outlet in the Numerical Model

6. NUMERICAL MODEL VALIDATION

In order to ensure that numerical simulations are close to reality, modeling results should be verified with laboratory results. For this purpose, in the present study, the pressure results obtained from numerical model of floor and duct wall from 30.7 m to the end of the bottom outlet at 80,60,40 and 20% service gate openings were compared with experimental results. The results of this comparison are presented in Figures 1 and 2. The measure of data error is the correlation coefficient (R^2), which is specified at the margin of each graph.



(P: Pressure, X: Distance from entrance)

Figure 4 Comparison mean pressure of the conduit floor from the numerical model with experimental results for different gate openings

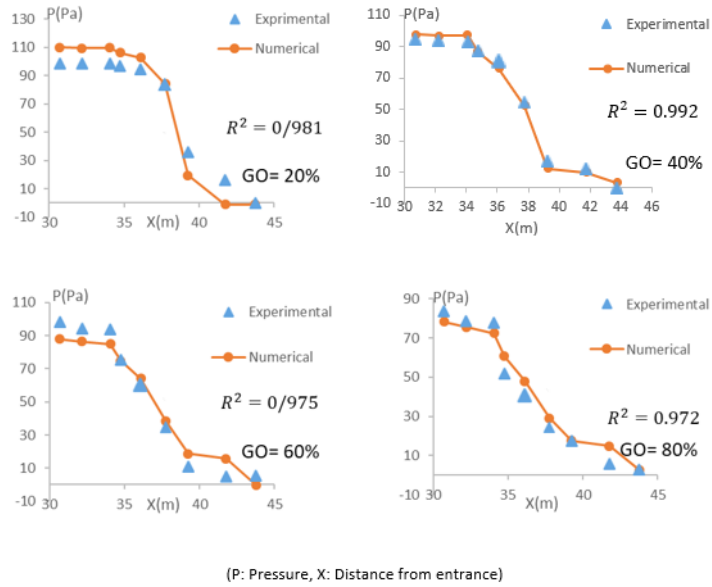


Figure 56 Comparison mean pressure of the conduit wall from the numerical model with experimental results for different gate openings

As can be seen from Figures 4 and 5, the results of the numerical model are slightly different from those of laboratory data, which can be due to measurement error in laboratory work or due to the lack of reservoir modeling and instead of using average velocity in model inlet. The maximum difference between the numerical and laboratory results is related to the vicinity of the gate, which can be due to Entering the flow into the air mixing zone and increasing turbulence in the area

7. RESULTS ANALYSIS

After solving the flow field numerically, the amount of air entered into the flow is investigated using the air concentration contour. From the air concentration contour near the conduit floor, it can be seen that at 10 and 20% openings, the flow does not contact the wall. At 30% openings, the flow does not contact the wall up to 5 meters after the gate. The 40% opening is the boundary between full contact and non-contact flow with the wall, so it has some properties of both cases so that it does not contact the wall at the beginning of opening of the section and then a small percentage of air enters into the flow in the form of cavities. In openings 60, 80 and 90% the flow in two centimeters of floor cover whole floor and there is a small percentage of air in some place. At a distance of four centimeters from the floor, in 80% and 90% openings, it can be seen that, a cavity of air which is surrounded by water enters into the flow. At 100% opening, cavity of air is created around the flow and up to a certain height prevents contact the wall with flow.

Concerning the concentration of air in the conduit wall, it can be said that in all openings there is no evidence of air bubbles spreading inside the flow on the wall. Air penetration into the flow is also restricted to the narrow band at the flow surface, with the exception of a 40% opening, which air is also seen slightly below the wall. In addition, it can be said that by increasing the service gate opening, the conduit wall comprises a larger area of flow, which the maximum of it is for 90% opening of the service gate. In 100% opening due to the presence of air cavity, the flow is only present in the middle part of the wall.

In general, it can be said that the aerator does not have the required efficiency to enter the bubble-shaped air into the flow and cannot be effective in reducing or counteracting the risk of cavitation, so that is why it needs redesign.

8. CONCLUSIONS

In this research, water-air two-phase flow by K- ϵ turbulence model and two-phase VOF model in FLUENT software has been modeled in 3D with the aim of evaluating the efficiency of wall aeration after bottom outlet service gate of Seymareh dam for normal reservoir head and different gate openings. Comparison between the results of numerical modeling and the laboratory data revealed that these results are in good agreement. After analyzing the flow field the results can be summarized as follows:

1- At the bottom of the conduit in small openings the air is present only at the flow boundary and in large openings the water flow covers the entire floor. At 90, 80 and 100% openings, there is also a cavity of air within the Output flow from the conduit.

2- On the conduit wall in all openings there is no trace of air bubbles spreading on the wall and the air penetration into the stream is limited to the narrow band at the flow surface.

3- Wall aerator after service gate does not have the required efficiency to enter the Bubble-shaped air into the flow and air is only seen at the flow boundary or as a air cavity in the flow. That this form of air intake cannot be effective in preventing the risk of cavitation. Therefore, aerator is not effective in preventing or reducing the risk of cavitation and requires redesign.

9. REFERENCES

1. Mohaghegh, A., & Wu, J. H. (2010). "Hydraulics of Discharge Tunnel Service Gate: the Flow Regimes". *Journal of Hydrodynamics*, 22(1), 692-698.
2. Li, S., Zhang, J., Chen, X., Zhou, G. G., & Chen, J. (2018). "Characteristics of Aeration in the Flow Downstream of a Radial Gate With a Sudden Fall-Expansion Aerator in a Discharge Tunnel". *Water Science and Technology: Water Supply*, 18(3), 790-798.
3. Hager, W. H. & Boes, R. M. 2014 Hydraulic structures: a positive outlook into the future. *Journal of Hydraulic Research* 52, 299–310. doi:10.1080/00221686.2014.923050.
4. Dong, Z. Y. & Su, P. L. 2006 Cavitation control by aeration and its compressible characteristics. *Journal of Hydrodynamics, Ser. B* 18 (4), 499–504. doi:10.1016/S1001-6058(06)60126-1.
5. Dong, Z. Y., Lei, C. & Ju, W. J. 2007 Cavitation characteristics of high velocity flow with and without aeration on the order of 50 m/s. *Journal of Hydrodynamics, Ser. B* 19 (4), 429–433. doi:10.1016/S1001-6058(07)60136-X
6. Zhang, J. M., Xu, W. L., Wang, W. & Liu, S. J. 2010 Cavitation damage to sidewalls in a sand flushing tunnel under high head. *J. Hydroelectr. Eng.* 29 (5), 197–201 (in Chinese)
7. Li, S., Zhang, J. M., Xu, W. L., Chen, J. G., Peng, Y., Li, J. N., & He, X. L. (2016). "Simulation and Experiments of Aerated Flow in Curve-Connective Tunnel with High Head and Large Discharge". *International Journal of Civil Engineering*, 14(1), 23-33.
8. Zhang, J. M., Chen, J. G., Xu, W. L., Wang, Y. R., & Li, G. J. (2011). "Three-dimensional Numerical Simulation of Aerated Flows Downstream Sudden Fall Aerator Expansion in a tunnel". *Journal of Hydrodynamics*, 23
9. Li, G. J., Dai, G. Q., Yang, Q., & Ma, X. D. (2011). "Detached Eddy Simulation of Hydraulic Characteristics along the Side-Wall after a New Arrangement-Scheme of the Sudden Lateral Enlargement and the Vertical Drop". *Journal of Hydrodynamics*, 23(5), 669-675
10. Hydraulic Model of seymareh dam bottom outlet (2005), Tehran Water Research Institute (in Persian)